Estuarine, Coastal and Shelf Science 301 (2024) 108757

Contents lists available at ScienceDirect

Estuarine, Coastal and Shelf Science

journal homepage: www.elsevier.com/locate/ecss

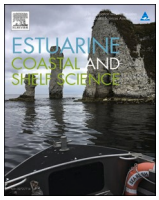

Patterns of marsh surface accretion rates along salinity and hydroperiod gradients between active and inactive coastal deltaic floodplains

Andy F. Cassaway [a,1], Robert R. Twilley [a], Andre S. Rovai [a,b,*], Gregg A. Snedden [c]

[a] Department of Oceanography and Coastal Sciences, College of the Coast and Environment, Louisiana State University, Baton Rouge, LA, 70803, USA
[b] U.S. Army Engineer Research and Development Center, Vicksburg, MS, 39183, USA
[c] U.S. Geological Survey, Wetland and Aquatic Research Center, Baton Rouge, LA, 70808, USA

ARTICLE INFO

Keywords:
Feldspar marker horizon
Mississippi river delta
Coastal wetlands
Relative tidal elevation
EVS-3
Delta-X

ABSTRACT

High subsidence rates are inherent to coastal deltas worldwide, contributing to rapid rates of relative sea-level rise and compromising the sustainability of coastal wetlands. Different parts of river deltas, however, experience accretion or erosion, depending on the coupling between ecological and morphological processes. Wetland expansion occurs in active deltaic coastal basins that are connected to riverine sedimentation. In contrast, wetland degradation occurs in inactive deltaic coastal basins where river engineering strategies associated with flood control restrict river connectivity. Here, we investigated the relative role of inorganic and organic loading to marsh accretion rates spanning fresh to brackish to saline zones between active and inactive coastal deltaic floodplains of the Mississippi River Delta. Marsh surface accretion rates monitored over 36 months using the feldspar marker horizon technique ranged from 1.24 ± 0.35 cm yr^{-1} in the freshwater marsh to 2.94 ± 0.51 cm yr^{-1} in the saline marsh in the inactive coastal basin compared to an opposite trend in the active coastal basin with a low vertical accretion rate in the saline site at 1.12 ± 0.17 cm yr^{-1} and higher accretion values at the freshwater site (2.14 ± 0.49 cm yr^{-1}). Our results suggest that saline marshes have high resilience identified by high vertical accretion rates exceeding those of river-dominated freshwater marshes in active deltaic floodplains. Overall, the marsh surface accretionary patterns detected in this study underscores the relative contribution of organic and inorganic sediments to elevation capital across salinity gradients between active and inactive basins in coastal Louisiana with particular interest to river management and restoration strategies. These findings, however, are applicable to coastal deltaic floodplains elsewhere given the repetition geomorphic forcings (e.g., relative contribution of riverine, tidal and wave power) and coastal typologies worldwide.

1. Introduction

Coastal wetlands are among the most productive environments on earth, also providing numerous benefits to society, including storm protection, nutrient removal, habitat value, and carbon sequestration (Barbier et al., 2011). These coastal ecosystem services are threatened as significant anthropogenic impacts cause 27% of recent wetland losses (Murray et al., 2022) associated with 40% of the global population occupying coastal environments (Williams et al., 2022). For example, many coastal landscapes are highly engineered to control river and tidal connectivity to provide flood control. Modifications such as river leveeing cut off sediment supply and alter adjacent wetlands' flooding frequency, duration and inundation level above marsh surface collectively termed hydroperiod (e.g., high engineered Mississippi River Delta coastal basins), which is a key factor for deltaic wetlands' survival relative to sea-level rise (Edmonds et al., 2023; Ensign et al., 2023).

The connectivity (frequency and volume of water exchange) of a wetland platform controls flooding regimes, allochthonous sediment supply and nutrient exchange, which altogether establish soil stressor gradients that can influence plant biomass productivity and allocation (e.g., root:shoot ratios) (Day et al., 2011a; Morris et al., 2002; Twilley et al., 2019). Above the marsh surface, wetlands plants' density (i.e., stems m^{-2}) and height reduce hydrodynamics and increase sediment deposition, reinforcing ecogeomorphic feedbacks that contribute to

* Corresponding author. Department of Oceanography and Coastal Sciences, College of the Coast and Environment, Louisiana State University, Baton Rouge, LA, 70803, USA.
E-mail address: andre.s.rovai@usace.army.mil (A.S. Rovai).
[1] Current affiliation: Coastal Design & Infrastructure Division, GIS Engineering, LLC, Baton Rouge LA 70801.

https://doi.org/10.1016/j.ecss.2024.108757
Received 10 August 2023; Received in revised form 29 March 2024; Accepted 5 April 2024
Available online 6 April 2024

surface vertical accretion (Nardin et al., 2016; Nardin and Edmonds, 2014). Beneath the marsh surface, root bio- and necromass productivity are key biotic controls on marsh platform elevation since organic matter adds an order of magnitude more volume to soils than mineral sediments (Morris et al., 2016; Morris and Sundberg, 2024). However, highly organic soils are more sensitive to changes in hydroperiod as organic matter deteriorates leading to sharp decreases in elevation capital (Morris et al., 2023). Altogether, organic matter production and inorganic sediment deposition, minus losses to decomposition, export, and subsidence, account for changes in wetland surface elevation determining whether the platform elevation – or elevation capital – can keep pace with relative sea-level rise (RSLR) (Herbert et al., 2021; Morris et al., 2016). And a decrease in elevation capital compared to RSLR results in the wetland being submerged, which can result in expansion of open water (Cahoon et al., 2020).

The Mississippi River Delta is composed of a mosaic of coastal deltaic floodplains in various stages of the delta cycle ranging in river and tidal connectivity, salinity variation, and platform elevation gradients, which provide avenues to examine how surface accretion processes vary across sediment (inorganic and organic) loading regimes. Avulsions of the Mississippi River historically induced connectivity with extensive areas of coastal deltaic floodplains, expanding emergent wetlands in coastal hydrologic basins as part of the active phase of the delta cycle (Bentley et al., 2016). Active coastal basins are characterized by a high degree of riverine connectivity where prograding deltaic landscapes form as a function of continuous sediment and nutrient availability that sustain plant-soil ecogeomorphic feedbacks (e.g., plant productivity and soil organic matter formation relative to elevation), maintaining surface elevation in steady state relative to mean sea level. In contrast, inactive coastal basins represent deltaic floodplains that have been disconnected from riverine sources, becoming prone to erosive forcings and subsidence in the absence of sediment input and gradual collapse in plant productivity following increased inundation time (Cahoon et al., 2020; Ma et al., 2018). While avulsions are a natural, self-organizing process of river-dominated coastal landscapes, modifications such as river damming and leveeing emulate and perpetuate conditions disruptive of the long-term sediment balance that maintains basin- and region-scale coastline stability (Twilley et al., 2016, 2019).

Along several of the Mississippi River's coastal basins, extensive levee systems and river control structures have emulated and intensified the natural inactive phase of the delta cycle by disconnecting wetlands from riverine sediment sources (Twilley et al., 2016). The Atchafalaya River conveys about 30% of the combined flow of the Mississippi and Red rivers to Atchafalaya Bay, and over time the Wax Lake and Atchafalaya deltas have emerged as a result of the accumulation of these fluvial materials (Wellner et al., 2005). The coastal wetlands near Fourleague Bay, an estuary in the distal region of Atchafalaya Bay, are inundated not only by tidal exchange, but also by seasonal peak river flow events (typically in spring) and routine winter storm forcing that promotes sediment resuspension from bay bottoms to adjacent wetlands (Perez et al., 2000; Restreppo et al., 2019; Wang et al., 2018). The Atchafalaya and Wax Lake deltas are active coastal floodplains that have exhibited increases in wetland area since 1974 (Wellner et al., 2005). Using an index of wetland:water areas to measure shoreline migration, this active coastal basin has a stable shoreline from 1932 to 2010 (Twilley et al., 2016). In contrast, Terrebonne Bay, just east of Atchafalaya Bay, represents an inactive coastal basin that has been disconnected from riverine sediment and has exhibited nearly 5000 km^2 (or ~25%) of wetlands loss between 1932 and 2016 (Couvillion et al., 2017). While wetland loss rates have decreased since a peak in the 1970's, the inactive coastal basins in Mississippi River Delta continue to experience negative rates of land area change each year (Couvillion et al., 2017). The landward migration of the shoreline in this inactive coastal basin has been 17 km from 1932 to 2010 as more marshes are converted to open-water (Couvillion et al., 2017; Twilley et al., 2016). However, it has been suggested that in such inactive coastal basins stable marshes regarded as 'land bridges' are maintained where there is enough fetch to promote wave-driven sediment resuspension that keeps elevation capital at or above current RSLR rates (Day et al., 2023).

Here, we used these two coastal basins to test how inorganic and organic sediment deposition varies with river sediment connectivity gradients in both the proximal and distal regions of an active (sediment-rich Atchafalaya Bay) and inactive (sediment-poor Terrebonne Bay) coastal deltaic floodplain (Fig. 1). Within each of these coastal basins, study sites were located along salinity gradients spanning freshwater, brackish, and saline intertidal zones. Using these experimental landscapes, we asked (1) What is the influence of inorganic and organic sediment loading in active vs. inactive coastal basins on marsh surface accretion rates? And (2) what is the relative role of inorganic and organic loading to marsh accretion rates at varying distances (proximal vs. distal) from river and marine sources? We hypothesized sedimentation rates to be lower in Terrebonne Bay coastal deltaic floodplains due to the lack of riverine sediment inputs, increased flooding (lower relative elevation) and susceptibility to salinity stress. We also expected sedimentation rates along the Atchafalaya Bay salinity transect to decrease from freshwater (proximal) to brackish to saline (distal) due to increased distance from the sediment source. However, we expected a reverse spatial trend in Terrebonne Bay with higher salinity distal locations having higher inorganic sediment input resulting from deposition of bay bottom resuspended loads during coastal frontal passages. Lastly, regarding factors influencing accretion rates, we posited that inorganic sedimentation would decrease with increasing relative tidal elevation due to reduced flooding and accommodation space.

2. Methods

2.1. Study sites and sampling strategy

Study sites were selected along salinity gradients (freshwater, brackish, and saline) within the Atchafalaya Bay (hereafter referred to as active basin or simply active) and Terrebonne Bay (hereafter inactive basin or inactive) as engineered hydrologic basins of the Mississippi River Delta Plain (Fig. 1). The active basin freshwater site is located on Mike Island of Wax Lake delta (WLD), which had higher intertidal elevations dominated by *Colocasia esculenta* and *Salix nigra*, and intermediate intertidal and subtidal zones by *Nelumbo lutea* and submerged aquatic vegetation (Bevington et al., 2022; Bevington and Twilley, 2018; Jensen et al., 2021; Rovai et al., 2022). The freshwater site in the inactive basin was dominated by *Persicaria punctata*, *Eleocharis montana*, and *Typha domingensis* (Castañeda-Moya and Solohin, 2022a). Brackish sites in both active and inactive basins were dominated by *Spartina patens* (Castañeda-Moya and Solohin, 2022a). Brackish and saline sites in the active basin were located in Fourleague Bay, an estuary in Atchafalaya Bay distal from the Atchafalaya River with distinct combination of river and tidal processes that control suspended sediment and nutrient loading to the adjacent marshes (Lane et al., 2011; Madden et al., 1988; Perez et al., 2000). Saline sites in both active and inactive basins were dominated by *Spartina patens* and *Spartina alterniflora* (Castañeda-Moya and Solohin, 2022a). Salinity zones were determined on the basis of dominant marsh communities, species composition and abundance (Nyman et al., 2022). For visualization purposes (Fig. 1), salinity marsh types reference GIS layers were retrieved from the Louisiana Coastal Protection and Restoration Authority (CPRA) Coastal Information Management System (CIMS) database (Nyman et al., 2022). Raster and vector manipulations were performed in using R packages 'raster' and 'rgdal' (Bivand et al., 2023; Hijmans, 2023; R Core Team, 2020).

2.2. Marsh surface accretion measurements and soil properties

Marsh surface total accretion rates and soil properties (bulk density, organic and inorganic matter content, and organic carbon content) were determined to assess differences in total, organic and inorganic surface

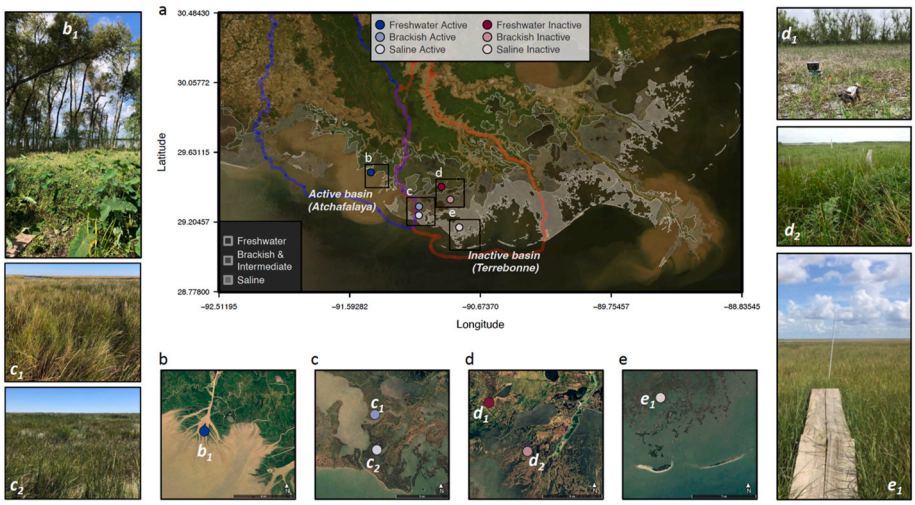

Fig. 1. Sampling sites (a–e) along freshwater (b_1, d_1), brackish (c_1, d_2) and saline (e_1) marshes in both sediment-rich active (blue outline) and sediment-poor inactive (red outline) coastal basins in Louisiana. Background image (a): True color Aqua-1 MODIS at 250 m pixel resolution taken on May 17th 2011, provided by Louisiana State University Earth Scan Laboratory and the University of Wisconsin-Madison Space Science and Engineering Center (Modified from Twilley et al., 2016). (b–e) Background image: Google Earth Pro v. 7.3.6.9345 Landsat/Copernicus 07/2023, accessed on 27 July 2023. Photos by A. Rovai, except d_2 and e_1, which were retrieved from https://lacoast.gov/crms_viewer/Map/CRMSViewer (Accessed on January 1, 2024). (For interpretation of the references to color in this figure legend, the reader is referred to the Web version of this article.)

vertical accretion and mass accumulation rates across studied sites. Marsh surface total accretion rates were measured using the feldspar marker horizon and liquid nitrogen cryocore technique to minimize compaction during sampling (Cahoon et al., 1996; Folse et al., 2018). Briefly, this technique accounts for total sediments (organic and inorganic) deposition on top a feldspar powder marker horizon previously laid over the marsh surface, which is gradually buried by autochthonous and allochthonous particles. At known time intervals, measurements of the vertical distance between soil surface deposits and the top of feldspar marker horizons (that is, the depth of accreted deposits) are used to estimate marsh surface total vertical accretion over time. Within each site, two replicate sampling stations, consisting of triplicate 50 × 50 cm feldspar marker horizon plots each, were deployed in October 2019, totaling twelve feldspar stations that were sampled at 12, 18, 24, 30, and 36 months (Fig. 1, Table 1). Sites were accessed by airboat, and a portable 2.5-m boardwalk was used to reach feldspar sampling stations to minimize disturbance of surrounding soil surfaces during sampling. Two cryocores were taken from two non-repeating, randomized plot locations in each of the triplicate feldspar plots at each sampling event. Each cryocore was measured three times with calipers to the nearest millimeter, and measurements were averaged to a singular accretion measurement per cryocore. In general, 6 cryocores per sampling station (totaling 12 cryocores per site) were retrieved depending on feldspar marker integrity assessed as clearly defined markers around cryocores. In some instances, however, fewer as 3–4 cryocores per sampling station were considered due to signs of bioturbation (e.g., bivalves burrowing, plant growth, animal tracks) or scouring. To account for the portion of the variability inherent to eventual uneven sampling caused by these natural, non-controllable events, multiple readings were recorded around viable cryocores and resulting marsh surface vertical accretion estimates were averaged at the feldspar plot level for each station and site within respective sampling campaigns.

Soil characteristics of recently accreted material were sampled adjacent to feldspar sampling stations to extend the lifetime of the feldspar marker horizons and minimize disturbance to the study area. For each cryocore sampled, a surface soil sample was collected using a Russian Peat Corer (AMS Inc., 5 cm internal diameter) matching the average depth of feldspar horizons observed on respective cryocores. Samples were transported to the laboratory on ice where they were temporarily stored at 4 °C, and subsequently oven-dried at 60 °C to constant mass. Soil bulk density was calculated on a gram of dry mass (gdm cm^{-3}) basis. Samples were then ground and passed through a 250 μm mesh for uniformity. Organic matter (OM) content (% dry mass) was determined by loss-on-ignition (LOI) where two analytical replicates were combusted at 550 °C for 2 h (Davies, 1974). Inorganic matter (IM) was calculated as % dry mass from OM content (IM = 100-OM). Organic

Table 1
Sampling strategy with sites nested within basins and number of replicate sampling units and measurements within feldspar marker horizon plots. Coastwide Reference Monitoring Stations (CRMS) are monitoring stations in coastal Louisiana managed by Coastal Protection and Restoration Authority (CPRA).

Basin	Site/Salinity zone	Longitude	Latitude	Replicate sampling station ID	Orthometric elevation m NAVD88 Geoid 12A (Mean±SE)
Active basin (Atchafalaya Bay)	Freshwater (Mike Island, Wax Lake delta, near CRMS0479)	29°30′32.11″N	91°26′40.33″W	A	−0.114 ± 0.007
		29°29′43.59″N	91°26′30.04″W	B	−0.054 ± 0.005
	Brackish (near CRMS0399)	29°17′57.48″N	91° 6′18.18″W	A	0.211 ± 0.004
		29°17′58.14″N	91° 6′17.28″W	B	0.254 ± 0.008
	Saline (near CRMS0322)	29°14′43.44″N	91° 6′22.86″W	A	0.191 ± 0.007
		29°14′44.34″N	91° 6′22.92″W	B	0.169 ± 0.009
Inactive basin (Terrebonne Bay)	Freshwater (near CRMS0294)	29°25′11.40″N	90°56′52.68″W	A	0.264 ± 0.009
		29°25′10.44″N	90°56′51.90″W	B	0.278 ± 0.010
	Brackish (near CRMS0396)	29°20′30.72″N	90°53′7.14″W	A	0.265 ± 0.007
		29°20′30.90″N	90°53′4.50″W	B	0.137 ± 0.013
	Saline (near CRMS0421)	29°10′17.22″N	90°49′21.24″W	A	0.123 ± 0.009
		29°10′18.18″N	90°49′20.82″W	B	0.037 ± 0.007

carbon (OC) content was determined by combusting two acid-fumigated (6 h exposure to 12M hydrochloric acid fumes; Harris et al., 2001) analytical replicates in an ECS 4010 elemental analyzer (Costech Analytical Technologies, Inc., Valencia, CA). IM, OM and OC densities (inorganic, organic matter and organic carbon mass per cm^3) were calculated on a volumetric basis using respective concentrations multiplied by sample bulk density (gdm cm^{-3}).

Marsh surface vertical accretion measurements recorded on top of feldspar marker horizons (3 readings for each cryocore, 2 cryocores for each feldspar plot) were averaged at the feldspar plot level for each station and site within respective sampling campaigns. Total, OM, IM, and OC mass accumulation rates (i.e., g m^{-2} yr^{-1}) were estimated as the product between these components' respective densities (g cm^{-3}) and vertical surface accretion rates (cm yr^{-1}). To capture both site-specific spatial and temporal variability, soil properties (bulk density, OM content and density, and OM, IM and OC mass accumulation rates) determined from soil samples collected adjacent to each feldspar station as described above were averaged at the feldspar plot level for each station and site across sampling campaigns. The volumetric contributions of organic and inorganic matter to marsh surface vertical accretion rates were determined by dividing site-specific organic and inorganic mass accumulation rates by respective soil bulk densities (Baustian et al., 2020).

Datum-referenced (NAVD88) hourly water level data and marsh surface elevations were used to determine the effect of elevation and flooding on marsh surface vertical accretion and mass accumulation rates across study sites. Hourly water level data collected from each of the nearby CRMS sites spanning Jan 2020–Dec 2022 were obtained from www.lacoast.gov/crms. This period was chosen to avoid biasing water level estimates by including only a partial year (that is, Nov and Dec 2019) during which water levels are typically below the annual average. Much of the water level data for CRMS0479 were missing, so water level at that station was imputed with a multiple linear regression model that predicted daily mean water level at CRMS0479 from the nearby NOAA Amerada Pass tide gauge (obtained from https://tidesandcurrents.noaa.gov) and Atchafalaya River discharge measured at Morgan City, LA (USGS 07381600; adjusted $r^2 = 0.95$). After using the model to obtain predictions of daily mean water level at CRMS0479, the daily data were linearly interpolated to an hourly time step, and the predicted lunar tide (obtained through harmonic analysis of water level data at CRMS0479) was added. The model was fit with data spanning 2010–2013, and the RMSE between predicted and observed values for 2014–2017 was 9 cm. The effect of elevation and flooding on marsh surface vertical accretion and sediment accumulation rates across salinity zone and basins was assessed on the basis of respective site-specific relative tidal elevations (Z*), which indicates the relative frequency, period, and depth of inundation during tidal cycles considering the tidal amplitude; see (Holmquist and Windham-Myers, 2021, 2022) for details). However, the range of the lunar tide along the northern Gulf of Mexico shelf is small (<1 m; Forbes, 1988) and much of the lunar tide's energy is dissipated as it progresses through the deltaic landscape (Snedden et al., 2007). As such, in many regions of coastal Louisiana most water level variation occurs over subtidal timescales and responds to lower-frequency forcing agents such as wind and river discharge variations that occur over weekly to seasonal timescales. Thus, metrics such as Z* that are based on the range of the lunar tide may be inappropriate to characterize a region where a large portion of water level variation occurs at subtidal timescales, and applying Z* to Gulf coast diurnal microtidal wetlands can result in uncertainties that exceed the tidal amplitude itself (Holmquist and Windham-Myers, 2022). To make our calculated relative tidal elevations (Z*) robust to these circumstances, we substituted the 90th percentile of the observed hourly water level measurements for the period Jan 2020–Dec 2022 and used it in place of the traditional mean high water to compute Z* (see equation 1 in (Holmquist and Windham-Myers, 2022). The resulting modified equation was: Z^* = [orthometric elevation - mean sea level]/[90th percentiles water levels - mean sea level]. Water level data were retrieved from the CPRA CRMS online repository (https://www.lacoast.gov/CRMS/), and marsh surface orthometric elevation was assessed at all feldspar sampling stations on November 2020 using a Real-Time Kinematic (RTK) Trimble R12 GPS and referenced to NAVD88 using the GEOID 12A model.

2.3. Statistical analyses

Simple linear regression models were fit to estimate marsh surface vertical accretion rates over the study period (Fall, 2019-Fall, 2022) for each site having net surface accretion measurements (in mm) as the dependent variable and time (in days) since feldspar marker horizons deployment as explanatory variable (Fig. 2).

A balanced hierarchical Analysis of Variance (ANOVA) design coupled with pairwise Student-Newman-Keuls (SNK) posthoc tests (both using the 'GAD' R package; Sandrini-Neto et al., 2014) were used to test for differences ($P < 0.05$) among sites nested within basins and between sites across basins (Supplementary Tables S1–S4). Basins were held as a fixed factor and sites as a random factor. Tests were run on either log-, cube root- or Box-Cox-transformed data to ensure residuals were normally distributed and homogeneity of variances were equal among groups (Underwood, 1997). Results are described as means ± 1SE unless stated otherwise.

3. Results

3.1. Marsh surface vertical accretion rates

In the active basin, surface vertical accretion rate (±1SE of estimate) was highest at the freshwater marsh estimated at 2.14 ± 0.49 cm yr^{-1} followed by saline and brackish marshes at 1.12 ± 0.17 and 0.78 ± 0.22 cm yr^{-1}, respectively (Fig. 2). Sites in the inactive basin had a different spatial trend in surface vertical accretion rates, increasing from 1.24 ± 0.35 cm yr^{-1} at freshwater marshes followed by 1.41 ± 0.52 and 2.94 ± 0.51 cm yr^{-1} at brackish and saline sites, respectively.

3.2. Marsh surface soil physicochemical properties and contribution of organic and inorganic mass to vertical accretion rates

In the active basin, bulk density was higher in the freshwater site (0.34 ± 0.03 g cm^{-3}) and similar between the brackish (0.17 ± 0.01 g cm^{-3}) and the saline (0.14 ± 0.01 g cm^{-3}) sites (Fig. 3a). In the inactive basin, bulk density significantly increased from freshwater (0.03 ± 0.002 g cm^{-3}) to brackish (0.08 ± 0.01 g cm^{-3}) to saline (0.17 ± 0.01 g cm^{-3}) sites. Accordingly, inorganic matter content decreased from freshwater (91.61 ± 0.31%) to brackish (72.06 ± 0.33%) to saline (64.21 ± 2.81%) sites in the active basin whereas in the inactive basin it increased with the salinity gradient (freshwater = 29.09 ± 0.96%, brackish = 59.32 ± 3.17%, saline = 78.74 ± 0.43%) (see Supplementary Tables S2 and S3 for ANOVA tables and posthoc tests results). Mirroring inorganic matter content, organic matter content had opposite trends between coastal basins, increasing from freshwater (8.38 ± 0.31%) to saline (35.79 ± 2.81%) site in the active basin and decreasing along this gradient in the inactive basin (freshwater = 70.90 ± 0.96%, brackish = 40.68 ± 3.17%, saline = 21.25 ± 0.43%) (Fig. 3b). Based on bulk density and OM content, OM density in the active basin was lower in the freshwater site (0.02 ± 0.001 g cm^{-3}) and similar between the brackish (0.04 ± 0.03 g cm^{-3}) and the saline (0.05 ± 0.03 g cm^{-3}) sites (Fig. 3c). In the inactive basin, OM density was equally lower at both freshwater and brackish sites (0.024 ± 0.001 and 0.029 ± 0.003 g cm^{-3}, respectively) and higher at the saline (0.035 ± 0.002 g cm^{-3}) site.

Inorganic mass accumulation rate was higher at the freshwater site (7248.3 ± 894.5 g m^{-2} yr^{-1}) relative to brackish and saline sites (975.9 ± 79.9 and 961.3 ± 91.5 g m^{-2} yr^{-1}) in the active basin while it increased from freshwater (128.4 ± 11.8 g m^{-2} yr^{-1}) to saline (4096.8 ± 317.5 g m^{-2} yr^{-1}) site in the inactive basin (Fig. 3d). Tracking

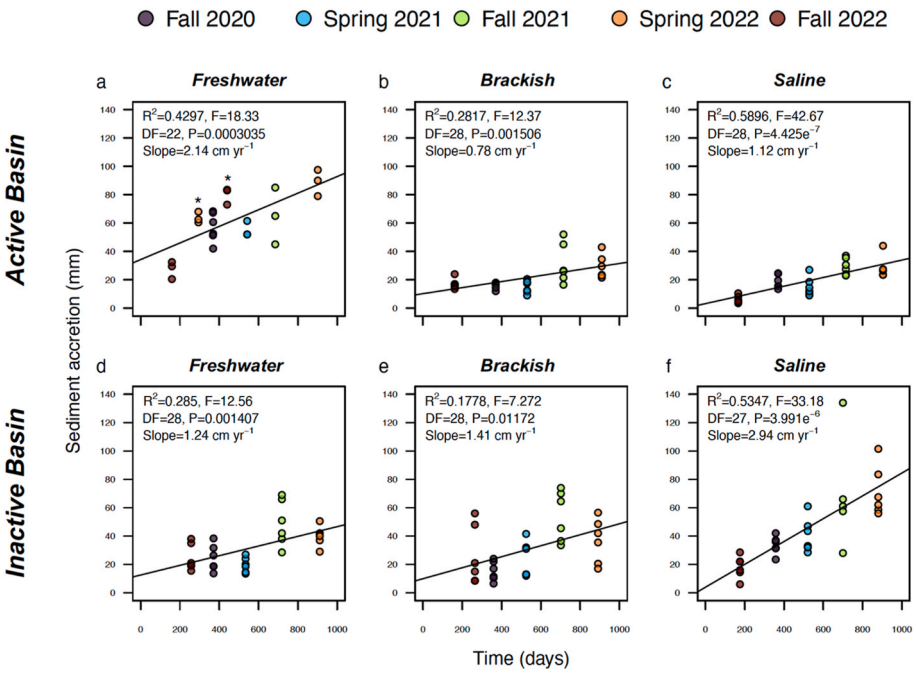

Fig. 2. Cumulative marsh surface vertical accretion rates estimated for freshwater (a,d), brackish (b,e) and saline (c,f) sites in both active (top panel row) and inactive (bottom panel row) coastal basins. Note that the Fall 2022 campaign has the least number of days since feldspar markers were redeployed during the Spring 2022 sampling campaign. Thus, Fall 2022 surface vertical accretion values are for 6–7 months old feldspar markers. In addition, asterisks on panel 'a' show feldspar stations that scoured during the course of the experiment and were redeployed within same site and sampled along with original stations through subsequent campaigns.

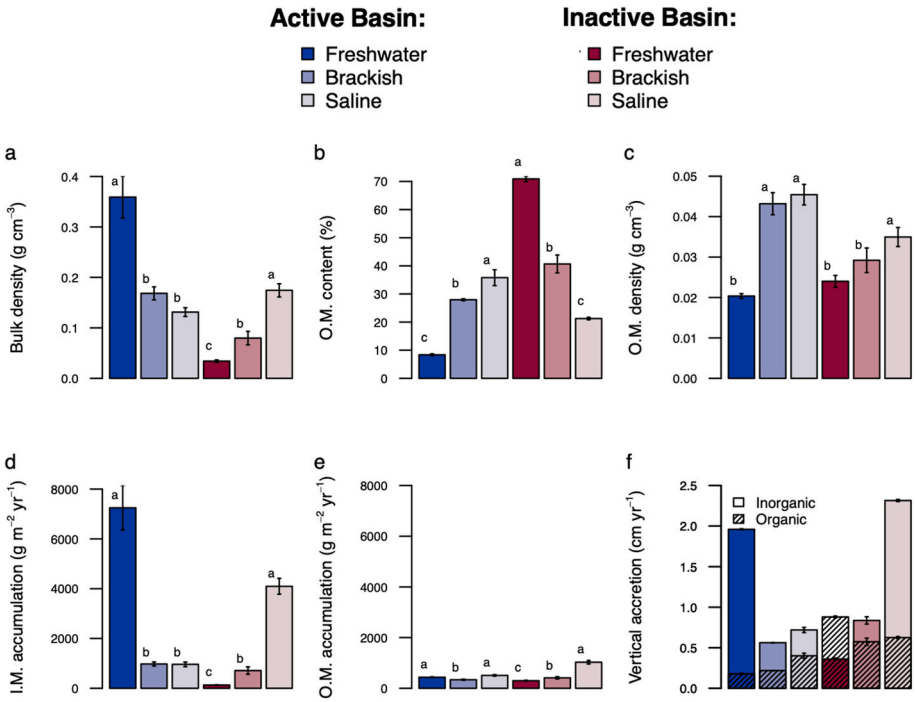

Fig. 3. (a) Soil bulk density, (b) organic matter (O.M.) content, (c) O.M. density, (d) inorganic matter (I.M.) accumulation rates, (e) O.M. accumulation rates, and (f) relative contribution of O.M. and I.M. to marsh surface vertical accretion across freshwater, brackish, and saline marshes in active and inactive coastal basins in Louisiana. Different lowercase letters on top of bars denote statistical differences for nested effects among sites within each basin.

inorganic mass accumulation rates, organic matter mass accumulation rates were higher in both freshwater (435.6 ± 12.5 g m^{-2} yr^{-1}) and saline (508 ± 28.3 g m^{-2} yr^{-1}) sites relative to the brackish (336 ± 21.3 g m^{-2} yr^{-1}) site in the active basin, whereas in the inactive basin OM mass accumulation rates increased from freshwater (297.5 ± 17.9 g m^{-2} yr^{-1}) to saline (1027.9 ± 69.1 g m^{-2} yr^{-1}) sites (Fig. 3e). Within both active and inactive basins OC accumulation rates were lower at both freshwater (150.5 ± 6.5 and 128.5 ± 7.5 g m^{-2} yr^{-1}, respectively) and brackish (143.2 ± 10.8 and 148.9 ± 10.4 g m^{-2} yr^{-1}, respectively) sites relative to saline (189.2 ± 13.1 and 367.0 ± 34.6 g m^{-2} yr^{-1},

respectively; Supplementary Tables S2 and S3). Reflecting these site-specific soil properties trends, the relative contribution of inorganic matter to marsh surface vertical accretion was highest at the freshwater active marsh followed by the saline inactive site while organic matter contributed for most of the vertical accretion in the freshwater and brackish inactive marshes (Fig. 3f).

3.3. Relative tidal elevation influence on surface accretion and mass accumulation rates

Relative tide elevation (Z*) in the active basin was lower in the freshwater marsh (Z*: −1.18 and −1.06) followed by brackish and saline (Z*: 0.02 and 0.13, and 0.13 and 0.16, respectively) sites (Fig. 4a). The highest surface vertical accretion and total mass (organic plus inorganic) accumulation rates were also observed at the active freshwater site (Fig. 4a–b). These higher rates seen at the active freshwater site are being mostly driven by higher IM mass accumulation rate as indicated by relatively higher bulk density and higher IM content (Fig. 3a and b). Contrary, in the inactive basin, relative tide elevation was lowest in the saline marsh (Z*: −0.74 and −0.58) followed by the brackish (Z*: −0.14, 0.17) and the freshwater sites (Z*: −0.12, −0.08) (Fig. 4a). However, in contrast to the active basin, the saline site in the inactive basin had the highest marsh surface vertical accretion and total mass accumulation rates relative to the brackish and the freshwater sites (Fig. 4a and b). Accordingly, higher marsh surface vertical accretion and total mass accumulation rates in the inactive saline site reflect deposition of substantial inorganic sediments as shown by higher bulk density and higher IM content, relative to brackish and freshwater sites (Fig. 3a and b). Further, an increase in tide range is observed in the freshwater site in the active basin (Fig. 4b) due to the influence of seasonal high river stage, which increases water levels across the riverine influenced region. This pattern is also noted for saline sites in both active and inactive basins (Fig. 4b) due to these sites' proximity to the Gulf of Mexico where tidal attenuation is lower and exposure to wind-driven changes in water levels is more pronounced. These patterns seem to be reflecting the relative positioning of these sites within the tidal frame, with both the freshwater site in the active basin and the saline site in the inactive basin being subjected to higher mean sea level, mean high and mean low water (Fig. 4c).

4. Discussion

The feldspar marker horizon technique accounts for cumulative net surface deposition of inorganic and organic sediments on the marsh surface that defines their relative contributions to marsh soil formation and net elevation change. Our experimental design with sites spanning salinity gradients nested within active and inactive coastal basins gives insight to the relative contribution of riverine, tidal, and meteorological forcings (Bevington et al., 2017) to surface sedimentation patterns reflecting contrasting phases of the delta cycle.

4.1. Patterns of surface accretion and mass accumulation rates in the active basin

Total mass (organic plus inorganic) accumulation rate in the freshwater active basin site was the highest observed across all studied sites, resulting from mostly allochthonous riverine sediment deposits characterized by high bulk densities and high inorganic matter content. Moreover, freshwater marshes in active basins are subjected to higher mean sea level (as well mean high and low water levels) due to additive effects of river discharge and tides (Fig. 4c), particularly during spring floods when the Atchafalaya River and Wax Lake outlet discharges elevate water levels at the delta front by 30–50 cm (Bevington et al., 2017), which increases the accommodation space available for river-borne particles to settle. Mostly riverine inorganic sediment loading has volumetrically built subaqueous and intertidal platforms that allowed for wetland plant communities to colonize and develop plant-soil feedbacks that further enhance elevation gain (Ma et al., 2018; Twilley et al., 2019). In addition to adding organic matter directly into the soil via root productivity, which increases soils' volume disproportionately relative to inorganic sediment inputs (Morris et al., 2016; Morris and Sundberg, 2024), wetland plants' aboveground structures promote hydrodynamic conditions conducive for sediments deposition, reinforcing net elevation gain feedbacks (Nardin et al., 2016; Nardin and Edmonds, 2014). Previous studies have shown that distinct freshwater marsh vegetation communities in active basins occupy discrete marsh platform elevation ranges (e.g., sub-, inter-, and supratidal zones; Bevington et al., 2022) whereas across inactive basins elevation ranges are mostly constricted to the mid intertidal zone (Table 1). In active basins, higher plant biomass (both above- and belowground) and soil organic matter were found in higher elevation profiles (high intertidal and supratidal), indicating that organic accretion becomes the primary

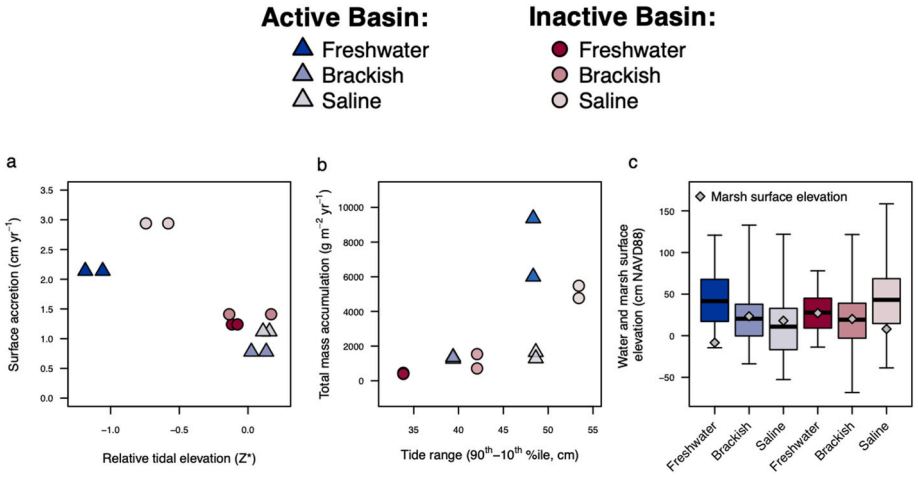

Fig. 4. (a) Marsh surface vertical accretion rates against relative tidal elevation (Z^* = [orthometric elevation - mean sea level]/[90th percentiles water levels - mean sea level]), (b) total mass (organic plus inorganic) accumulation rates relative to tide range computed from 10th and 90th percentiles of water levels used as proxies for mean low and mean high water levels (see Methods section for details), and (c) water levels across sampling sites for the period Jan 2020–Dec 2022. Boxplots were customized to show mean sea levels (horizontal thick line), 10th and 90th water levels percentiles (bottom and top of boxes, respectively), and minimum and maximum water levels (whiskers). Gray diamonds show marsh surface orthometric elevation values for each site.

biotic control of elevation change as flooding duration and mineral sediment loading decreases whereas inorganic accretion prevails in subtidal and low intertidal zones (Bevington and Twilley, 2018; Jensen et al., 2021; Rovai et al., 2022). While we have constrained our study sites to the intertidal hydrogeomorphic zone (Table 1), we have not directly assessed the role of vegetation structure on marsh surface and subsurface (e.g., root zone) total accretion, which should be further scrutinized given that plants' density and biomass distribution unequivocally affect soil accretionary dynamics (Brückner et al., 2019; Cahoon et al., 2020; Nyman et al., 1993). However, net marsh surface vertical accretion and total mass accumulation rates assessed in this study are site-specific observations, thus, a function of distinct vegetation communities that both affect and are adapted to local hydrology.

In the distal portion of the active basin, brackish and saline marsh sites exhibited reduced surface vertical accretion rates due to these sites' protected locations inside Fourleague Bay, an estuarine embayment in the lower Atchafalaya Bay (Twilley et al., 2019). The sheltered positioning of these sites to fetch likely results in reduced wave resuspension of bay bottom sediments and may explain the lower vertical accretion rates relative to sites closer to open water bodies where deposition of wave resuspended sediments are more intense (Cortese and Fagherazzi, 2022). However, the connectivity with riverine sediments from both Wax Lake outlet and the Atchafalaya River, evident from river plumes observed across Vermillion, Atchafalaya, and Fourleague bays, formed what has been described as a large river delta estuary (Bianchi and Allison, 2009). This connectivity with riverine sources is reflected in extremely high total suspended solids in Fourleague Bay waters during high river flood pulse and frontal passages, when the suspended sediment load flooding adjacent marshes ranges from 500 to 2000 mg L^{-1} (Day et al., 2011a). Further, brackish and saline sites in the active basin are positioned higher within the tidal frame with relative tidal elevations above mean sea level (Fig. 4a), which enhances sediment retention due to increased tidal drainage and consolidation of newly layered soil cohorts, resulting in net surface elevation gain (Day et al., 2011a; Twilley et al., 2016). The higher bulk density and lower organic matter content observed on recently deposited sediments in these active brackish and saline sites (Fig. 3a and b) match the higher inorganic suspended sediment fraction in observed in Fourleague Bay waters relative to those noted for the inactive basin water bodies (Day et al., 2011a; Rovai et al., 2022; Wang et al., 1993). These findings reflect the important role of fluvial subsidies in maintaining multi-decadal shoreline stability spanning proximal across coastal deltaic floodplain landscapes (Twilley et al., 2016).

4.2. Patterns of surface accretion and mass accumulation rates in the inactive basin

Contrary to trends observed in the active basin, the inactive basin saline site had significantly higher sedimentation rates, which may reflect this site's proximity to the open waters of Terrebonne Bay. In the inactive basin both vertical sediment accretion and total (organic and inorganic) mass accumulation rates increased from the proximal to distal regions along the freshwater to saline transect. The increased fetch associated with inactive basins as observed in Terrebonne Bay provides the sufficient energy to resuspend bay bottom sediments that are subsequently deposited on saline marsh platforms (Cortese and Fagherazzi, 2022; Karimpour et al., 2017; Liu et al., 2018), forming land bridges in deltaic landscapes (Day et al., 2023). Much of inorganic sediment loading to bay bottoms of the inactive basin are derived from wave-induced marsh edge erosion (Sapkota and White, 2019; Wilson and Allison, 2008), and to a much lesser extent from strongly diluted Mississippi River plume waters driven into the bay during easterly wind events (Allahdadi et al., 2011) or tidal exchange (Ou et al., 2020). Indeed, these bay bottom sediments are generally low in organic content since a significant fraction of this pool is rapidly mineralized in the aerobic estuarine water following marsh edge erosion-driven resuspension (Sapkota and White, 2021). Moreover, our inactive basin saline site is positioned lower in the intertidal frame within open bays facing the Gulf of Mexico where accommodation space is amplified by increased hydroperiod allowing for larger loads of suspended sediments to settle (Rogers et al., 2019). On the contrary, both more interiorized brackish and freshwater marshes in the inactive basin had nearly half the surface vertical accretion rate observed at the saline site since they receive less storm-driven sediment deposition (Cortese and Fagherazzi, 2022). Along with restricted upstream sediment transport due to tide attenuation decreasing from the Gulf of Mexico inland (Snedden and Steyer, 2013), this diminished connectivity with episodic sediment loading events has been proposed as an important driver of substantial marsh area loss for inland regions of coastal Louisiana's inactive basins (Day et al., 2023). Noteworthy, tropical storms can also contribute to coastal wetlands' soil surface vertical accretion (Bevington et al., 2017; Breithaupt et al., 2020; Castañeda-Moya et al., 2020; Feher et al., 2019; Smith et al., 2015). However, while the seven named storms that occurred in the Gulf of Mexico over the duration of our experiment (Laura, Sally, Beta, Delta and Zeta in 2020, and Ida and Nicholas in 2021) have temporarily raised water levels at our sites by up to ~90 cm above historical mean high water levels (Supplementary Fig. S1), no discernible effect on observed marsh surface vertical accretion rates was perceptible as seen in our linear regression models (Fig. 2).

Also important to maintaining marsh surface elevation in steady state relative to RSLR, in situ organic matter productivity increases soil volume by an order of magnitude relative to inorganic sediments due to higher porosity (Morris et al., 2016; Morris and Sundberg, 2024). Indeed, high soil organic matter density values observed across all inactive basin sites are due to increased belowground biomass productivity, particularly at the saline marsh in response to relatively higher soil N:P ratios (Castañeda-Moya and Solohin, 2022b), higher salinity levels (Alldred et al., 2017), and increasingly created accommodation space triggered by loss of elevation capital (Cahoon et al., 2020; Saintilan et al., 2022; Turner et al., 2002). However, reduced soil conditions caused by prolonged flooding stimulates the formation of aerenchyma tissue, which in turn reduces root mechanical strength (Striker et al., 2007). Further, while voluminous aerenchyma may build elevation more rapidly, their higher root porosity can lead to faster organic matter collapse and rapid elevation loss following flood-induced mortality (Morris et al., 2023; Striker et al., 2007). Therefore, while autochthonous sediment supply (i.e., organic and/or locally resuspended mineral matter) plays an important role to maintain marsh vertical accretion in low total suspended matter coastal settings such as inactive basins (Saintilan et al., 2022), these land bridge marshes tend to degrade if not stabilized against wave-driven edge erosion (Cortese and Fagherazzi, 2022; Day et al., 2023) or connection to a continuous riverine sediment supply is not enhanced (Edmonds et al., 2023). Lastly, the spatial patterns described in this study recapitulate those noted for Venice lagoon in Italy, a composite river-wave dominated system part of the Po delta, where higher sedimentation rates have been observed near the river mouth (source of sediments) and along high wave energy shorelines where marsh surface deposits resulted from resuspended bottom sediments (Day et al., 1999, 2011b). Further, the combination of high wave energy and lack of sediment was also identified as the main driver for wetland loss to sea-level rise in Venice lagoon (Day et al., 1999). These similarities reflect the repetition of coastal processes operating across analogous coastal typologies worldwide (Boyd et al., 1992; Thom et al., 1975; Woodroffe et al., 2016), supporting the broader applicability of our study design and findings, and reinforcing the land bridge marshes concept as a universal framework for engineering strategies to anticipate and adapt to rising sea levels (Day et al., 2023).

5. Conclusions

Our results show that saline marshes in inactive delta basins exhibit high vertical accretion rates which exceed those of river-dominated

freshwater marshes in active coastal basins. This is likely due to sediment sourced from open bays with large wind fetch that are resuspended during storms and subsequently available for surface deposition on adjacent marsh platforms, particularly those situated low in the intertidal frame as shown elsewhere (Cortese and Fagherazzi, 2022; Karimpour et al., 2017; Liu et al., 2018). However, unsteady and insufficient fluvial sediment supply (Edmonds et al., 2023) and high rates of wave-driven erosion have been suggested as detrimental to maintaining elevation capital (Cortese and Fagherazzi, 2022) under subsidence rates twice as high as sea-level rise (RSLR rates along Louisiana's coast ranging from 6 to 9 mm year^{-1}; Törnqvist et al., 2020), culminating in rapid land loss rates as historically documented for the studied region. Overall, the marsh surface accretionary patterns detected in this study underlines the relative contribution of organic and inorganic sediments to elevation capital across salinity gradients between active and inactive basins in coastal Louisiana with particular interest to river management and restoration strategies. These findings, however, are applicable to coastal deltaic floodplains elsewhere given the repetition geomorphic forcings (e.g., relative contribution of riverine, tidal and wave power) and coastal typologies worldwide.

Funding

The NASA Delta-X project (https://deltax.jpl.nasa.gov) is funded by the Science Mission Directorate's Earth Science Division through the Earth Venture Suborbital-3 Program NNH17ZDA001N-EVS3.

CRediT authorship contribution statement

Andy F. Cassaway: Writing – review & editing, Writing – original draft, Project administration, Methodology, Investigation, Formal analysis, Data curation. **Robert R. Twilley:** Writing – review & editing, Supervision, Resources, Project administration, Methodology, Investigation, Funding acquisition, Conceptualization. **Andre S. Rovai:** Writing – review & editing, Writing – original draft, Visualization, Validation, Supervision, Project administration, Methodology, Investigation, Formal analysis, Data curation, Conceptualization. **Gregg A. Snedden:** Writing – review & editing, Visualization, Validation, Formal analysis.

Declaration of competing interest

The authors declare the following financial interests/personal relationships which may be considered as potential competing interests: Andre Scarlate Rovai reports financial support was provided by NASA.

Data availability

The marsh surface accretion rates and soil properties dataset used in this study is available at https://doi.org/10.3334/ORNLDAAC/2079

Acknowledgements

We are thankful to the Louisiana Department of Wildlife and Fisheries, ConocoPhillips and Apache Minerals for granting site access permits, as well as to Thomas Blanchard with the Louisiana State University's Wetlands Biogeochemistry and Analytical Services (https://www.lsu.edu/cce/research/labs/wbas.php) for support with laboratory analytical work. Any use of trade, firm, or product names is for descriptive purposes only and does not imply endorsement by the U.S. Government.

Appendix A. Supplementary data

Supplementary data to this article can be found online at https://doi.org/10.1016/j.ecss.2024.108757.

References

Allahdadi, M.N., Jose, F., Stone, G.W., D'Sa, E.J., 2011. The fate of sediment plumes discharged from the Mississippi and Atchafalaya Rivers: an integrated observation and modeling study for the Louisiana shelf, USA. In: The Proceedings of the Coastal Sediments 2011. World Scientific Publishing Company, pp. 2212–2225. https://doi.org/10.1142/9789814355537_0166.

Alldred, M., Liberti, A., Baines, S.B., 2017. Impact of salinity and nutrients on salt marsh stability. Ecosphere 8, e02010. https://doi.org/10.1002/ecs2.2010.

Barbier, E., Hacker, S., Kennedy, C., Koch, E., Stier, A., Silliman, B., 2011. The value of estuarine and coastal ecosystem services. Ecol. Monogr. 81 (2), 169–193.

Baustian, M.M., Reed, D., Visser, J., Duke-Sylvester, S., Snedden, G., Wang, H., DeMarco, K., Foster- Martinez, M., Sharp, L.A., McGinnis, T., Jarrell, E., 2020. 2023 coastal Master plan: Attachment D2: ICM-wetlands. Vegetation, and Soil Model Improvements. Version 2. Baton Rouge.

Bentley, S.J., Blum, M.D., Maloney, J., Pond, L., Paulsell, R., 2016. The Mississippi River source-to-sink system: Perspectives on tectonic, climatic, and anthropogenic influences, Miocene to Anthropocene. Earth Sci. Rev. 153, 139–174. https://doi.org/10.1016/j.earscirev.2015.11.001.

Bevington, A.E., Twilley, R.R., 2018a. Island edge Morphodynamics along a Chronosequence in a prograding deltaic floodplain wetland. J. Coast Res. https://doi.org/10.2112/JCOASTRES-D-17-00074.1.

Bevington, A.E., Twilley, R.R., 2018b. Island edge Morphodynamics along a Chronosequence in a prograding deltaic floodplain wetland. J. Coast Res. https://doi.org/10.2112/JCOASTRES-D-17-00074.1.

Bevington, A.E., Twilley, R.R., Sasser, C.E., 2022a. Deltaic floodplain wetland vegetation dynamics along the sediment surface elevation gradient and in response to disturbance from river flooding and hurricanes in Wax Lake Delta, Louisiana, USA. Geomorphology 398, 108011. https://doi.org/10.1016/j.geomorph.2021.108011.

Bevington, A.E., Twilley, R.R., Sasser, C.E., 2022b. Deltaic floodplain wetland vegetation dynamics along the sediment surface elevation gradient and in response to disturbance from river flooding and hurricanes in Wax Lake Delta, Louisiana, USA. Geomorphology 398, 108011. https://doi.org/10.1016/j.geomorph.2021.108011.

Bevington, A.E., Twilley, R.R., Sasser, C.E., Holm, G.O., 2017a. Contribution of river floods, hurricanes, and cold fronts to elevation change in a prograding deltaic floodplain in the northern Gulf of Mexico, USA. Estuar. Coast Shelf Sci. 191, 188–200. https://doi.org/10.1016/j.ecss.2017.04.010.

Bevington, A.E., Twilley, R.R., Sasser, C.E., Holm, G.O., 2017b. Contribution of river floods, hurricanes, and cold fronts to elevation change in a prograding deltaic floodplain in the northern Gulf of Mexico, USA. Estuar. Coast Shelf Sci. 191, 188–200. https://doi.org/10.1016/j.ecss.2017.04.010.

Bianchi, T.S., Allison, M.A., 2009. Large-river delta-front estuaries as natural "recorders" of global environmental change. Proc Natl Acad Sci U S A 106, 8085–8092. https://doi.org/10.1073/pnas.0812878106.

Bivand, R., Keitt, T., Rowlingson, B., 2023. Rgdal: Bindings for the "Geospatial" data Abstraction Library_. R package version 1, 6–7.

Boyd, R., Dalrymple, R., Zaitlin, B.A., 1992. Classification of clastic coastal depositional environments. Sediment. Geol. 80, 139–150. https://doi.org/10.1016/0037-0738(92)90037-R.

Breithaupt, J.L., Smoak, J.M., Bianchi, T.S., Vaughn, D., Sanders, C.J., Radabaugh, K.R., Osland, M.J., Feher, L.C., Lynch, J.C., Cahoon, D.R., Anderson, G.H., Whelan, K.R.T., Rosenheim, B.E., Moyer, R.P., Chambers, L.G., 2020. Increasing rates of carbon burial in southwest Florida coastal wetlands. J. Geophys. Res.: Biogeosciences. https://doi.org/10.1029/2019JG005349.

Brückner, M.Z.M., Schwarz, C., van Dijk, W.M., van Oorschot, M., Douma, H., Kleinhans, M.G., 2019. Salt marsh establishment and eco-engineering effects in dynamic estuaries determined by species growth and mortality. J Geophys Res Earth Surf 124, 2962–2986. https://doi.org/10.1029/2019JF005092.

Cahoon, D.R., Lynch, J.C., Knaus, R.M., 1996. Improved cryogenic coring device for sampling wetland soils. J. Sediment. Res. 66, 1025–1027. https://doi.org/10.2110/jsr.66.1025.

Cahoon, D.R., McKee, K.L., Morris, J.T., 2020. How plants influence resilience of salt marsh and mangrove wetlands to sea-level rise. Estuar. Coast 44, 883–898. https://doi.org/10.1007/s12237-020-00834-w.

Castañeda-Moya, E., Rivera-Monroy, V.H., Chambers, R.M., Zhao, X., Lamb-Wotton, L., Gorsky, A., Gaiser, E.E., Troxler, T.G., Kominoski, J.S., Hiatt, M., 2020. Hurricanes Fertilize Mangrove Forests in the Gulf of Mexico (Florida Everglades, USA), vol. 117. Proceedings of the National Academy of Sciences, pp. 4831–4841. https://doi.org/10.1073/pnas.1908597117.

Castañeda-Moya, E., Solohin, E., 2022a. Delta-X: aboveground biomass and necromass across wetlands, MRD, Louisiana, 2021. https://doi.org/10.3334/ORNLDAAC/2000.

Castañeda-Moya, E., Solohin, E., 2022b. Delta-X: soil properties for Herbaceous wetlands, MRD, Louisiana, 2021. https://doi.org/10.3334/ORNLDAAC/2078.

Cortese, L., Fagherazzi, S., 2022a. Fetch and distance from the bay control accretion and erosion patterns in Terrebonne marshes (Louisiana, USA). Earth Surf. Process. Landforms 47, 1455–1465. https://doi.org/10.1002/esp.5327.

Cortese, L., Fagherazzi, S., 2022b. Fetch and distance from the bay control accretion and erosion patterns in Terrebonne marshes (Louisiana, USA). Earth Surf. Process. Landforms 47, 1455–1465. https://doi.org/10.1002/esp.5327.

Couvillion, B.R., Beck, H., Schoolmaster, D., Fischer, M., 2017. Land Area Change in Coastal Louisiana (1932 to 2016), vol. 3381. U.S. Geological Survey Scientific Investigations Map, Reston, Virginia.

Davies, B.E., 1974. Loss-on-Ignition as an estimate of soil organic matter. Soil Sci. Soc. Am. J. 38, 150–151. https://doi.org/10.2136/sssaj1974.03615995003800010046x.

Day, J., Ibáñez, C., Scarton, F., Pont, D., Hensel, P., Day, Jason, Lane, R., 2011a. Sustainability of mediterranean deltaic and lagoon wetlands with sea-level rise: the importance of river input. Estuar. Coast 34, 483–493. https://doi.org/10.1007/s12237-011-9390-x.

Day, J.W., Kemp, G.P., Reed, D.J., Cahoon, D.R., Boumans, R.M., Suhayda, J.M., Gambrell, R., 2011b. Vegetation death and rapid loss of surface elevation in two contrasting Mississippi delta salt marshes: the role of sedimentation, autocompaction and sea-level rise. Ecol. Eng. 37, 229–240. https://doi.org/10.1016/j.ecoleng.2010.11.021.

Day, J.W., Rybczyk, J., Scarton, F., Rismondo, A., Are, D., Cecconi, G., 1999. Soil accretionary dynamics, sea-level rise and the survival of wetlands in Venice Lagoon: a field and modelling approach. Estuar. Coast Shelf Sci. 49, 607–628. https://doi.org/10.1006/ecss.1999.0522.

Day, J.W., Twilley, R.R., Freeman, A., Couvillion, B., Quirk, T., Jafari, N., Mariotti, G., Hunter, R., Norman, C., Kemp, G.P., White, J.R., Meselhe, E., 2023. The concept of land bridge marshes in the Mississippi River Delta and implications for coastal restoration. Nature-Based Solutions 3, 100061. https://doi.org/10.1016/j.nbsj.2023.100061.

Edmonds, D.A., Toby, S.C., Siverd, C.G., Twilley, R., Bentley, S.J., Hagen, S., Xu, K., 2023. Land loss due to human-altered sediment budget in the Mississippi River Delta. Nat. Sustain. https://doi.org/10.1038/s41893-023-01081-0.

Ensign, S.H., Halls, J.N., Peck, E.K., 2023. Watershed sediment cannot offset sea level rise in most US tidal wetlands. Science 382, 1191–1195. https://doi.org/10.1126/science.adj0513.

Feher, L.C., Osland, M.J., Anderson, G.H., Vervaeke, W.C., Krauss, K.W., Whelan, K.R.T., Balentine, K.M., Tiling-Range, G., Smith, T.J., Cahoon, D.R., 2019. The long-term effects of hurricanes Wilma and Irma on soil elevation change in Everglades mangrove forests. Ecosystems. https://doi.org/10.1007/s10021-019-00446-x.

Folse, T.M., West, J.L., Hymel, M.K., Troutman, J.P., Sharp, A., Weifenbach, D., Mcginnis, T., Rodrigue, L.B., 2018. A Standard Operating Procedures Manual for the Coast-wide Reference Monitoring System- Wetlands.

Forbes, M.J., 1988. Hydrologic investigations of the lower Calcasieu river, Louisiana, water-Resources Investigations report. Baton Rouge, LA. https://doi.org/10.3133/wri874173.

Harris, D., Horwáth, W.R., van Kessel, C., 2001. Acid fumigation of soils to remove carbonates prior to total organic carbon or Carbon-13 isotopic analysis. Soil Sci. Soc. Am. J. 65, 1853–1856. https://doi.org/10.2136/sssaj2001.1853.

Herbert, E.R., Windham-Myers, L., Kirwan, M.L., 2021. Sea-level rise enhances carbon accumulation in United States tidal wetlands. One Earth 4, 425–433. https://doi.org/10.1016/j.oneear.2021.02.011.

Hijmans, R.J., 2023. Raster: Geographic data analysis and modeling. R package version 3, 6–23.

Holmquist, J.R., Windham-Myers, L., 2022. A conterminous USA-scale map of relative tidal marsh elevation. Estuar. Coast 45, 1596–1614. https://doi.org/10.1007/s12237-021-01027-9.

Holmquist, J.R., Windham-Myers, L., 2021. Relative tidal marsh elevation maps with uncertainty for conterminous USA, 2010. https://doi.org/10.3334/ORNLDAAC/1844.

Jensen, D., Cavanaugh, K.C., Simard, M., Christensen, A., Rovai, A., Twilley, R., 2021. Aboveground biomass distributions and vegetation composition changes in Louisiana's Wax Lake Delta. Estuar. Coast Shelf Sci. 250, 107139 https://doi.org/10.1016/j.ecss.2020.107139.

Karimpour, A., Chen, Q., Twilley, R.R., 2017. Wind wave behavior in fetch and depth limited estuaries. Sci. Rep. 7, 40654 https://doi.org/10.1038/srep40654.

Lane, R.R., Madden, C.J., Day, J.W., Solet, D.J., 2011. Hydrologic and nutrient dynamics of a coastal bay and wetland receiving discharge from the Atchafalaya river. Hydrobiologia 658, 55–66. https://doi.org/10.1007/s10750-010-0468-4.

Liu, K., Chen, Q., Hu, K., Xu, K., Twilley, R.R., 2018. Modeling hurricane-induced wetland-bay and bay-shelf sediment fluxes. Coast. Eng. 135, 77–90. https://doi.org/10.1016/j.coastaleng.2017.12.014.

Ma, H., Larsen, L.G., Wagner, R.W., 2018. Ecogeomorphic feedbacks that Grow deltas. J Geophys Res Earth Surf 123, 3228–3250. https://doi.org/10.1029/2018JF004706.

Madden, C.J., Day, J.W., Randall, J.M., 1988. Freshwater and marine coupling in estuaries of the Mississippi River deltaic plain. Limnol. Oceanogr. 33, 982–1004. https://doi.org/10.4319/lo.1988.33.4part2.0982.

Morris, J.T., Barber, D.C., Callaway, J.C., Chambers, R., Hagen, S.C., Hopkinson, C.S., Johnson, B.J., Megonigal, P., Neubauer, S.C., Troxler, T., Wigand, C., 2016. Contributions of organic and inorganic matter to sediment volume and accretion in tidal wetlands at steady state. Earth's Future 4, 110–121. https://doi.org/10.1002/2015EF000334.

Morris, J.T., Langley, J.A., Vervaeke, W.C., Dix, N., Feller, I.C., Marcum, P., Chapman, S. K., 2023. Mangrove trees outperform saltmarsh grasses in building elevation but collapse rapidly under high rates of sea-level rise. Earth's Future 11, e2022EF003202. https://doi.org/10.1029/2022EF003202.

Morris, J.T., Sundareshwar, P.V., Nietch, C.T., Kjerfve, B.B., Cahoon, D.R., 2002. Responses of coastal wetlands to rising sea level. Ecology 83, 2869–2877. https://doi.org/10.2307/3072022.

Morris, J.T., Sundberg, K., 2024. Responses of coastal wetlands to rising sea-level revisited: The importance of organic production. Estuar. Coast. https://doi.org/10.1007/s12237-023-01313-8.

Murray, N.J., Worthington, T.A., Bunting, P., Duce, S., Hagger, V., Lovelock, C.E., Lucas, R., Saunders, M.I., Sheaves, M., Spalding, M., Waltham, N.J., Lyons, M.B., 2022. High-resolution mapping of losses and gains of Earth's tidal wetlands. Science (1979) 376, 744–749.

Nardin, W., Edmonds, D.A., 2014. Optimum vegetation height and density for inorganic sedimentation in deltaic marshes. Nat. Geosci. 7, 722–726. https://doi.org/10.1038/ngeo2233.

Nardin, W., Edmonds, D.A., Fagherazzi, S., 2016. Influence of vegetation on spatial patterns of sediment deposition in deltaic islands during flood. Adv. Water Resour. 93, 236–248. https://doi.org/10.1016/j.advwatres.2016.01.001.

Nyman, J.A., DeLaune, R.D., Roberts, H.H., Patrick, W.H., 1993. Relationship between vegetation and soil formation in a rapidly submerging coastal marsh. Mar. Ecol. Prog. Ser. 96, 269–279. https://doi.org/10.3354/meps096269.

Nyman, J.A., Reid, C.S., Sasser, C.E., Linscombe, J., Hartley, S.B., Couvillion, B.R., Villani, R.K., 2022. Vegetation Types in Coastal Louisiana in 2021.

Ou, Y., Xue, Z.G., Li, C., Xu, K., White, J.R., Bentley, S.J., Zang, Z., 2020. A numerical investigation of salinity variations in the Barataria Estuary, Louisiana in connection with the Mississippi River and restoration activities. Estuar. Coast Shelf Sci. 245, 107021 https://doi.org/10.1016/j.ecss.2020.107021.

Perez, B.C., Day, J.W., Rouse, L.J., Shaw, R.F., Wang, M., 2000. Influence of Atchafalaya River discharge and winter frontal passage on suspended sediment concentration and flux in Fourleague Bay, Louisiana. Estuar. Coast Shelf Sci. 50, 271–290. https://doi.org/10.1006/ecss.1999.0564.

R Core Team, 2020. R: A Language and Environment for Statistical Computing.

Restreppo, G.A., Bentley, S.J., Wang, J., Xu, K., 2019. Riverine sediment contribution to distal deltaic wetlands: Fourleague bay, LA. Estuar. Coast 42, 55–67. https://doi.org/10.1007/s12237-018-0453-0.

Rogers, K., Kelleway, J.J., Saintilan, N., Megonigal, J.P., Adams, J.B., Holmquist, J.R., Lu, M., Schile-Beers, L., Zawadzki, A., Mazumder, D., Woodroffe, C.D., 2019. Wetland carbon storage controlled by millennial-scale variation in relative sea-level rise. Nature 567, 91–95. https://doi.org/10.1038/s41586-019-0951-7.

Rovai, A.S., Twilley, R.R., Christensen, A., McCall, A., Jensen, D.J., Snedden, G.A., Morris, J.T., Cavell, J.A., 2022a. Biomass allocation of tidal freshwater marsh species in response to natural and manipulated hydroperiod in coastal deltaic floodplains. Estuar. Coast Shelf Sci. 268, 107784 https://doi.org/10.1016/j.ecss.2022.107784.

Rovai, A.S., Twilley, R.R., Christensen, A., McCall, A., Jensen, D.J., Snedden, G.A., Morris, J.T., Cavell, J.A., 2022b. Biomass allocation of tidal freshwater marsh species in response to natural and manipulated hydroperiod in coastal deltaic floodplains. Estuar. Coast Shelf Sci. 268, 107784 https://doi.org/10.1016/j.ecss.2022.107784.

Saintilan, N., Kovalenko, K.E., Guntenspergen, G., Rogers, K., Lynch, J.C., Cahoon, D.R., Lovelock, C.E., Friess, D.A., Ashe, E., Krauss, K.W., Cormier, N., Spencer, T., Adams, J., Raw, J., Ibanez, C., Scarton, F., Temmerman, S., Meire, P., Maris, T., Thorne, K., Brazner, J., Chmura, G.L., Bowron, T., Gamage, V.P., Cressman, K., Endris, C., Marconi, C., Marcum, P., Laurent, K.St., Reay, W., Raposa, K.B., Garwood, J.A., Khan, N., 2022. Constraints on the adjustment of tidal marshes to accelerating sea level rise. Science (1979) 377, 523–527. https://doi.org/10.1126/science.abo7872.

Sandrini-Neto, L., Gilbert, E.R., Camargo, M.G., 2014. R Package GAD: Analysis of Variance from General Principles.

Sapkota, Y., White, J.R., 2021. Long-term fate of rapidly eroding carbon stock soil profiles in coastal wetlands. Sci. Total Environ. 753, 141913 https://doi.org/10.1016/j.scitotenv.2020.141913.

Sapkota, Y., White, J.R., 2019. Marsh edge erosion and associated carbon dynamics in coastal Louisiana: a proxy for future wetland-dominated coastlines world-wide. Estuar. Coast Shelf Sci. 226, 106289 https://doi.org/10.1016/j.ecss.2019.106289.

Smith, J.E., Bentley, S.J., Snedden, G.A., White, C., 2015. What role do hurricanes play in sediment Delivery to subsiding river deltas? Sci. Rep. 5 https://doi.org/10.1038/srep17582.

Snedden, G.A., Cable, J.E., Wiseman, W.J., 2007. Subtidal sea level variability in a shallow Mississippi River deltaic estuary, Louisiana. Estuar. Coast 30, 802–812. https://doi.org/10.1007/BF02841335.

Snedden, G.A., Steyer, G.D., 2013. Predictive occurrence models for coastal wetland plant communities: Delineating hydrologic response surfaces with multinomial logistic regression. Estuar. Coast Shelf Sci. 118, 11–23. https://doi.org/10.1016/j.ecss.2012.12.002.

Striker, G.G., Insausti, P., Grimoldi, A.A., Vega, A.S., 2007. Trade-off between root porosity and mechanical strength in species with different types of aerenchyma. Plant Cell Environ. 30, 580–589. https://doi.org/10.1111/j.1365-3040.2007.01639.x.

Thom, B.G., Wright, L.D., Coleman, J.M., 1975. Mangrove ecology and deltaic-estuarine geomorphology: cambridge gulf-ord river, western Australia. J. Ecol. 63, 203–232. https://doi.org/10.2307/2258851.

Törnqvist, T.E., Jankowski, K.L., Li, Y., González, J.L., 2020. Tipping points of Mississippi Delta marshes due to accelerated sea-level rise. Sci. Adv. 6, eaaz5512.

Turner, R., Swenson, E., Milan, C., 2002. Organic and inorganic contributions to vertical accretion in salt marsh sediments. In: Concepts and Controversies in Tidal Marsh Ecology. Springer, pp. 583–595. https://doi.org/10.1007/0-306-47534-0_27.

Twilley, R.R., Bentley, S.J., Chen, Q., Edmonds, D.A., Hagen, S.C., Lam, N.S.-N., Willson, C.S., Xu, K., Braud, D., Hampton Peele, R., McCall, A., 2016. Co-evolution of wetland landscapes, flooding, and human settlement in the Mississippi River Delta Plain. Sustain. Sci. 11, 711–731. https://doi.org/10.1007/s11625-016-0374-4.

Twilley, R.R., Day, J.W., Bevington, A.E., Castañeda-Moya, E., Christensen, A., Holm, G., Heffner, L.R., Lane, R., McCall, A., Aarons, A., Li, S., Freeman, A., Rovai, A.S., 2019. Ecogeomorphology of coastal deltaic floodplains and estuaries in an active delta: insights from the Atchafalaya Coastal Basin. Estuar. Coast Shelf Sci. 227, 106341 https://doi.org/10.1016/j.ecss.2019.106341.

Underwood, A.J., 1997. Experiments in Ecology: Their Logical Design and Interpretation Using Analysis of Variance. Cambridge University Press, Cambridge, U.K.

Wang, E.C., Tiesong, Lu, Sikora, W.B., 1993. Intertidal marsh suspended sediment transport processes, Terrebonne Bay, Louisiana, USA. J. Coast Res. 9, 209–220.

Wang, J., Xu, K., Restreppo, G.A., Bentley, S.J., Meng, X., Zhang, X., 2018. The coupling of bay hydrodynamics to sediment transport and its implication in micro-tidal wetland sustainability. Mar. Geol. 405, 68–76. https://doi.org/10.1016/j.margeo.2018.08.005.

Wellner, R., Beaubouef, R., Van Wagoner, J., Roberts, H.H., Sun, T., 2005. Jet-plume depositional bodies - the primary building blocks of Wax Lake Delta. Gulf Coast Association of Geological Societies Transactions 55, 867–909.

Williams, B.A., Klein, C.J., Roberson, L.A., Kuempel, C.D., Watson, J.E.M., Beyer, H.L., Montgomery, J., Runting, R.K., Grantham, H.S., Halpern, B.S., Wenger, A., Frazier, M., Venter, O., 2022. Global rarity of intact coastal regions. Conserv. Biol. 1–12. https://doi.org/10.1111/cobi.13874.

Wilson, C.A., Allison, M.A., 2008. An equilibrium profile model for retreating marsh shorelines in southeast Louisiana. Estuar. Coast Shelf Sci. 80, 483–494. https://doi.org/10.1016/j.ecss.2008.09.004.

Woodroffe, C.D., Rogers, K., McKee, K.L., Lovelock, C.E., Mendelssohn, I.A., Saintilan, N., 2016. Mangrove sedimentation and response to relative sea-level rise. Ann. Rev. Mar. Sci 8, 243–266. https://doi.org/10.1146/annurev-marine-122414-034025.